ELSEVIER

Journal of Alloys and Compounds 356–357 (2003) 142–146

Journal of ALLOYS AND COMPOUNDS

www.elsevier.com/locate/jallcom

Crystallographic and magnetic structure of $Pr_6Fe_{13}AuD_{13}$

V.A. Yartys[a], F.R. de Boer[b], K.H.J. Buschow[b,*], B. Ouladdiaf[c], H.W. Brinks[a], B.C. Hauback[a]

[a]*Institute for Energy Technology, P.O. Box 40, Kjeller, N 2027, Norway*
[b]*Van der Waals-Zeeman Institute, University of Amsterdam Valckenierstr. 65, 1018 XE Amsterdam, The Netherlands*
[c]*Institute Laue-Langevin, B.P. 156, 38042 Grenoble Cedex 9, France*

Received 1 June 2002; accepted 25 October 2002

Abstract

Neutron diffraction performed on deuterated powder samples of $Pr_6Fe_{13}Au$ shows that the crystal structure of the parent compound is retained upon charging with deuterium. The refined composition of the deuteride is $Pr_6Fe_{13}AuD_{13}$. The deuterium atoms occupy various types of interstitial sites bounded by Pr and Fe atoms. Each of these sites is surrounded by at least two Pr atoms. A collinear antiferromagnetic ordering of the four Fe and the two Pr sublattices was reported previously for the uncharged $Pr_6Fe_{13}Au$ compound. By contrast, a collinear ferromagnetic structure has been derived from the present neutron data of the deuteride. The easy moment direction is the same in $Pr_6Fe_{13}AuD_{13}$ and $Pr_6Fe_{13}Au$, being perpendicular to the **c**-axis. For the deuteride this result was derived from a complementary synchrotron radiation X-ray study made on magnetically aligned particles of the ferromagnetic deuteride.

Keywords: Hydrogen storage materials; Gas–solid reactions; Neutron diffraction; X-ray synchrotron diffraction; Crystal structure and symmetry

1. Introduction

Rare earth compounds of the type $R_6Fe_{13}X$ (X=Cu, Ag, Au, Si, Sn, etc.) form only for the first few members of the rare earth series. They crystallise in the tetragonal $Nd_6Fe_{13}Si$-type structure (space group $I4/mcm$) [1,2]. This structure is an ordered variant of the $La_6Co_{11}Ga_3$ structure [3] with two rare earth sites R1 ($16l$) and R2 ($8f$) and four Fe sites Fe1 ($16l_1$), Fe2 ($16k$), Fe3 ($16l_2$) and Fe4 ($4d$). Magnetic measurements have shown that the magnetic ordering of these compounds is antiferromagnetic (AF) with fairly high Néel temperatures, typically around 400 K [4,5], also confirmed by Mössbauer spectroscopy [6–8].

Neutron diffraction performed on powder samples of several of these compounds revealed a collinear AF ordering of the four Fe and two R sublattices associated with the wave vector $\mathbf{q}=(001)$ [5]. The moments of all sublattices located at ($xy0$) layers, sandwiched between successive X layers perpendicular to **c** at z −0.25 and 0.25 are confined to the same direction within the ($xy0$) plane. They revert their direction collectively when going to the next X layers at $z=0.25$, 0.75. The R moments at 1.5 K are generally smaller than their free-ion values while the average Fe ordered value is 2.2 μ_B/Fe, in agreement with Mössbauer results.

The $R_6Fe_{13}X$ compounds easily absorb fairly large amounts of hydrogen leading to drastic changes of their magnetic properties [4,9]. In the present investigation we have charged the $Pr_6Fe_{13}Au$ compound with deuterium for neutron diffraction experiments. The purpose of our investigation is to determine the crystallographic location of the D atoms and to determine the magnetic structure of the deuteride.

2. Experimental

The $Pr_6Fe_{13}Au$ sample was prepared by arc melting starting materials of at least 99.9% purity, using an excess of about 2% of Pr. After annealing for about 3 weeks at 1070 K, the sample was quenched to room temperature. X-ray diffraction diagrams showed that the sample was approximately single phase ($Nd_6Fe_{13}Si$ type structure).

The synthesis of the deuteride was performed at deuterium pressures not exceeding 2 bar using deuterium gas with a purity of 99.8%. The starting alloy was initially activated by annealing in a dynamic vacuum at 600 K for 30 min. After activation, the sample was cooled to room

---

*Corresponding author. Tel.: +31-20-525-5714; fax: +31-20-525-5788.
E-mail address: buschow@science.uva.nl (K.H.J. Buschow).

0925-8388/02/$ – see front matter © 2002 Elsevier B.V. All rights reserved.
doi:10.1016/S0925-8388(02)01222-7

Table 1
Experimental conditions for the powder neutron diffraction experiments

	λ (Å)	2θ interval (°)	Step $\Delta 2\theta$ (°)	T (K)
PUS	1.555	10–130	0.05	293
D1B	2.524	5.5–85.3	0.2	2–300 K (temperature scan) 2 and 300 K (measurements with high statistics)
D2B	1.591	5–162	0.05	2 and 300 K

temperature and deuterium was injected into the stainless steel autoclave. The deuteration started instantly and proceeded exothermically with high speed until saturation at the composition $Pr_6Fe_{13}AuD_{13}$. For the neutron diffraction studies the deuteride was reloaded from the autoclave into a vanadium sample holder with diameter 5 mm. The handling of the deuteride was carried out in a glovebox under a purified argon atmosphere.

Synchrotron powder X-ray diffraction (SR PXD) data for $Pr_6Fe_{13}Au$ and $Pr_6Fe_{13}AuD_{13}$ were collected in the Debye–Scherrer mode with the powder diffractometer at the Swiss–Norwegian Beam Line BM1 at ESRF, Grenoble. Monochromatic X-rays with wavelengths $\lambda=0.50056$ and 0.50095 Å were used. The samples were contained in rotating sealed glass capillaries of 0.3-mm diameter. A magnetic field of 1 T was applied perpendicular to the direction of the capillary during the measurements of the deuteride.

Powder neutron diffraction (PND) data were collected with the PUS instrument at JEEP II reactor (Kjeller) and with the D1B and D2B diffractometers at ILL, Grenoble. Measurements were performed at 293 K (PUS, D1B and D2B) and at 2 K using the yellow ILL type cryostat (D1B and D2B). Details of the experimental conditions employed are summarized in Table 1.

The GSAS [10] program was used in the refinements of the nuclear structure from powder diffraction data. The FULLPROF [11] program was employed in the refinement of the magnetic structure.

3. Experimental results and discussion

In a previous neutron diffraction investigation of $Pr_6Fe_{13}Au$ it was shown that the magnetic ordering involves collinear antiferromagnetic ordering of the four Fe sublattices and the two Pr sublattices with a propagation vector $\mathbf{q}=(001)$ [5]. The prominent feature of the neutron pattern was the appearance of a very strong magnetic peak (001), around $2\theta=5°$ ($\lambda=1.9114$ Å), offering the possibility to determine the easy moment direction in the antiferromagnet as being perpendicular to the **c**-axis. This peak is totally absent in the PND pattern of the deuteride $Pr_6Fe_{13}AuD_{13}$. Because of the ferromagnetic nature of $Pr_6Fe_{13}AuD_{13}$ and its tetragonal symmetry, the easy magnetic moment direction as parallel or perpendicular to the **c**-axis can be distinguished. Alignment of the powder particles of the ferromagnetic sample in the magnetic field offers the possibility to derive the easy moment directions from X-ray diffraction. High brilliance synchrotron radiation at ESRF revealed differences between the diffractograms of the free sample and the sample aligned in a field of 1 T, indicating that the directions of the magnetic moments in the deuteride are perpendicular to the **c**-axis.

Table 2
Atomic positional parameters, site occupation numbers and characteristics of the interstitial sites obtained from the Rietveld refinements of the neutron diffraction data from $Pr_6Fe_{13}AuD_{13}$ powder sample at 300 K (PUS instrument)

Atom	x	y	z	Occupancy	Surrounding of interstitial sites[a]
Pr1 (16*l*)	0.1686(12)	0.6686(12)	0.1878(4)	1(–)	
Pr2 (8*f*)	0	0	0.0962(7)	1(–)	
Fe1 ($16l_1$)	0.1746(7)	0.6746(7)	0.0532(2)	1(–)	
Fe2 (16*k*)	0.0635(10)	0.2169(8)	0	1(–)	
Fe3 ($16l_2$)	0.6135(6)	0.1135(6)	0.0883(2)	1(–)	
Fe4 (4*d*)	0	1/2	0	1(–)	
Au (4*a*)	0	0	1/4	1(–)	
D1 (8*g*)	1/2	0	0.1353(8)	0.775(24)	T $(Pr1)_2(Fe3)_2$
D2 (16*l*)	0.3700(14)	−0.1300(14)	0.2191(6)	0.706(15)	T $(Pr1)_4$
D3 (4*c*)	1/2	1/2	0	1.000(–)	O $(Pr2)_2$ $(Fe2)_4$
D4 (32*m*)	0.0770(17)	0.2308(14)	0.1391(4)	0.715(16)	T $(Pr1)_2(Pr2)(Fe3)$
D5 (32*m*)	0.2022(–)	0.1980(–)	0.1054(–)	0.173(15)	T (Pr1)(Pr2)(Fe1)(Fe3)
D6 (32*m*)	0.2720(–)	0.0560(–)	0.1070(–)	0.082(15)	T (Pr1)(Pr2)(Fe1)(Fe3)

Space group *I*4/*mcm*. Lattice constants: $a=8.1735(8)$ Å, $c=25.408(4)$ Å.

[a] O, octahedron; T, tetrahedron.

Table 3
Magnetic moments (in μ_B per atom) derived from the refinement of the neutron diffraction data of $Pr_6Fe_{13}AuD_{13}$ (D1B instrument) and $Pr_6Fe_{13}Au$ at various temperatures

Atom	$Pr_6Fe_{13}Au$ [5]	$Pr_6Fe_{13}AuD_{13}$ [a]	$Pr_6Fe_{13}Au$ [5]	$Pr_6Fe_{13}AuD_{13}^{*}$
	293 K AF	300 K FM	1.5 K AF	2 K FM
Pr1 (16*l*)	0.6	0.5	2.6	1.7
Pr2 (8*f*)	1.7	2.7	2.6	2.5
Fe1 ($16l_1$)	1.7	1.7	2.4	3.4
Fe2 (16*k*)	1.5	1.9	2.6	1.7
Fe3 ($16l_2$)	1.4	0.0	2.2	1.6
Fe4 (4*d*)	1.1	0.8	0.8	2.2

The data of $Pr_6Fe_{13}Au$ were taken from Ref. [5].
[a] Average standard deviation ±0.3 μ_B.

The neutron diffraction patterns collected at 2 and 300 K show almost the same peaks. At $T=300$ K, all the observed peaks are indexed in the $Nd_6Fe_{13}Si$-type structure (space group *I4/mcm*). The magnetic contribution, which is superposed to the nuclear one, increases with decreasing the temperature. The corresponding propagation vector is $\mathbf{k}=(000)$. The refinement of the neutron pattern leads to a ferromagnetic arrangement with magnetic moments perpendicular to the **c**-axis. The ferromagnetic arrangement is in agreement with results of magnetic measurements reported elsewhere for the hydrides of the $R_6Fe_{13}X$ compounds [4,9]. Results of the refinement are reported in Tables 2 and 3. The neutron pattern obtained with D1B at 2 K (Fig. 1), shows in addition to the peaks at 300 K, a very weak reflection at $2\theta=18.7°$, indexed as (101). This peak is forbidden in space group *I4/mcm* and indicates the presence of a very small AF component, also with a propagation vector $\mathbf{k}=(000)$. Since the intensity of this peak is relatively weak and due to the large number of magnetic sites, it is not possible to reveal further details of this AF component. The refinement of the neutron pattern at 2 K, when neglecting this AF component, shows also a main ferromagnetic component in the (**a**,**b**) plane. A schematic representation of the crystal structure is shown in Fig. 2. The total magnetic moment increases from 22.8 μ_B at room temperature to 40.9 μ_B at 2 K (in agreement with magnetisation data [9]).

The magnetic moments from the previous PND study of $Pr_6Fe_{13}Au$ [5] are compared with the deuteride in Table 3. It is noteworthy that the Pr1 atoms located at the 16*l* position have a very small moment at room temperature, both in the deuteride and in the parent compound. This behaviour may be understood from the location of this Pr site, leading to a lower Pr–Fe coupling than for the Pr2 moments at the 8*f* site. Due to the increasing Pr–Pr coupling, the Pr1 moments increase, though, at lower temperatures, albeit they still remain smaller that the Pr2 moments.

The magnetic moment of the Fe3 atoms containing the highest number of D atoms in their surrounding (7) compared to the other Fe atoms (0–4 atoms D), is very small (or even zero) at room temperature. The reason for this is the comparatively low number of Fe nearest neighbours (7) and the comparatively high number of Pr

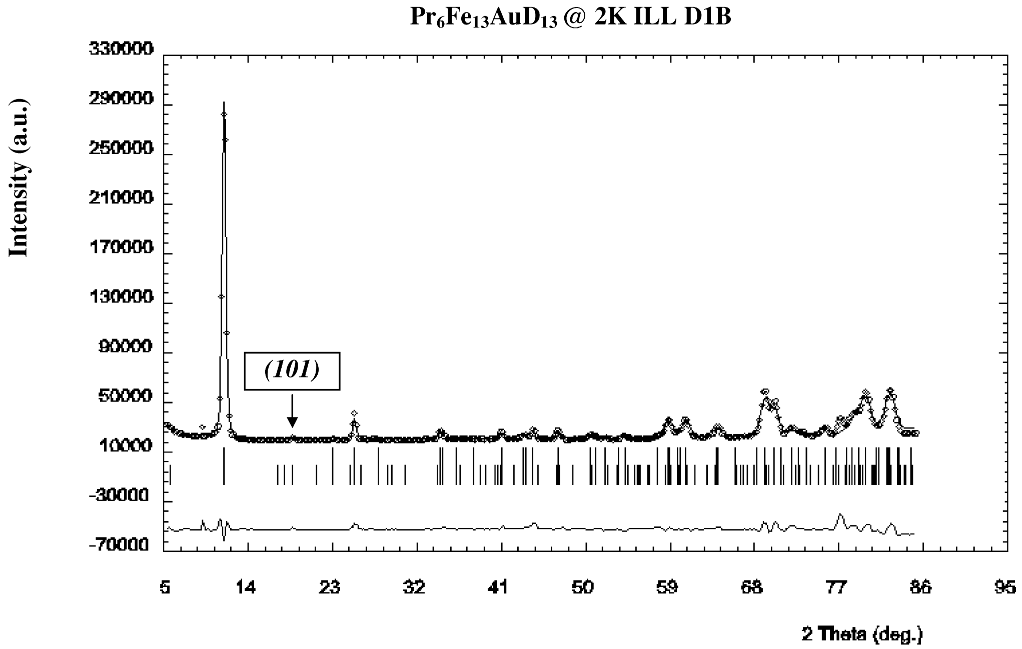

Fig. 1. Neutron diffraction diagram obtained at 2 K containing observed (diamonds), calculated (full line) and difference pattern of $Pr_6Fe_{13}AuD_{13}$ at 2 K ($R_p=4.35\%$; $R_{wp}=6.22\%$; $R_{magn}=7.19\%$). The positions of the nuclear (top) and magnetic (bottom) Bragg reflections are shown with bars below the diffraction pattern for the nuclear (upper) and magnetic (bottom) contributions. The (101) reflection (shown on a plot) appears in the data below 50 K ($2\theta=18.7°$).

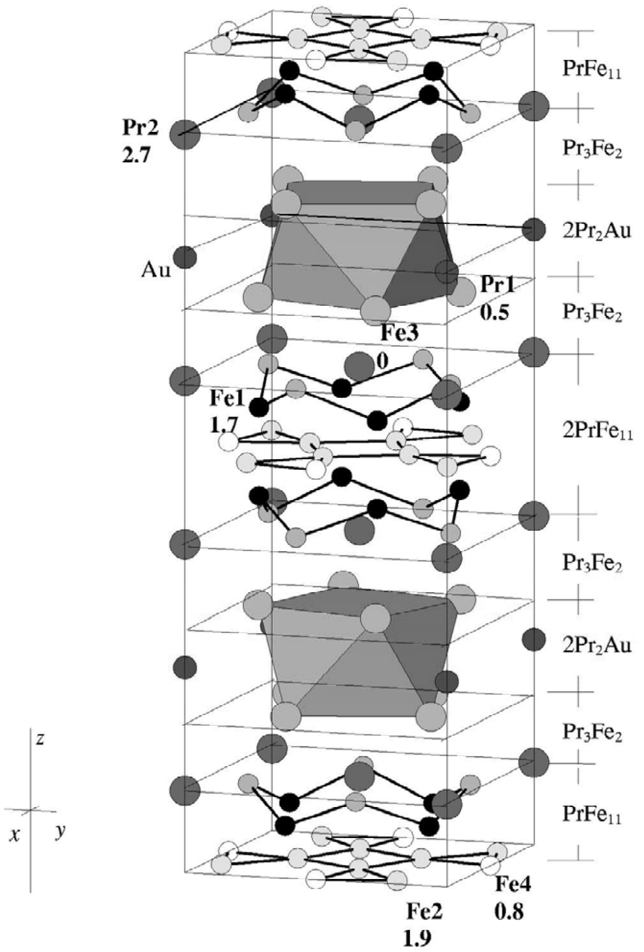

Fig. 2. Schematic representation of the crystal structures of $Pr_6Fe_{13}AuD_{13}$. Only the metal atoms are shown with the moment size at 300 K (in μ_B) for the various Fe and Pr sites.

nearest neighbours (5). The majority of the Pr nearest neighbours (3) consists of the Pr1 atoms, which are almost not magnetically ordered at room temperature. When these become ordered at low temperatures also the Fe3 atoms adopt magnetic moments.

Characteristics of the interstitial sites occupied by the deuterium atoms and the corresponding occupation numbers have been collected in Table 2. The overall composition of the deuteride corresponding to the refined occupation numbers is $Pr_6Fe_{13}AuD_{13.1}$. From the lattice constants for the deuteride (Table 2) and the parent intermetallic compound $Pr_6Fe_{13}Au$ ($a=8.09918(8)$, $c=22.6753(3)$ Å), the volume expansion is calculated to be $\Delta V=210.0$ Å^3, or equivalently $\Delta V/V=0.142$. These values are slightly smaller than for hydrogenated $Pr_6Fe_{13}Au$ [9].

The structure of $Pr_6Fe_{13}Au$ can be visualised as being composed of slabs with different chemical compositions, Pr_2Au, Pr_3Fe_2 and $PrFe_{11}$, stacked along [1] (see Fig. 2). By deuteration, the structure expands predominantly along the stacking direction of these slabs. As expected, the latter expansions, $\Delta c/c$, are very dissimilar for the various slabs. There is quite a significant expansion of 16.3% for Pr_2Au and 29.8% for Pr_3Fe_2, and with a slight contraction of −2.9% for $PrFe_{11}$. The differences originate from different deuterium content in these three slabs. The highest deuterium concentration is reached in the Pr_3Fe_2 slab. Only one deuterium occupied site, D3, is located in the $PrFe_{11}$ layer.

Table 2 shows a strong preference for the deuterium atoms to occupy the interstitial sites formed by praseodymium and iron. In contrast, none of the Au-surrounded sites is filled with D. Complete occupancy by D is observed for the only available octahedral site, Pr_2Fe_4 (D3). Five occupied tetrahedral sites have occupancies ranging from comparatively high 70–75% (D1, D2, D4) to much smaller values 8–17% (D5, D6), depending on the slab they occupy (D1, D4, Pr_3Fe_2; D2, border between Pr_2Au and Pr_3Fe_2; D5 and D6, border between Pr_3Fe_2 and $PrFe_{11}$). It is interesting to note that all occupied interstitial hole sites are bounded by at least two Pr atoms. From energy considerations one would expect that the higher the number of rare earth atoms surrounding a given interstitial site, the higher its occupation. This is only partially in keeping with the results presented in Table 2. It shows that the volumes of the interstitial holes and the nearest neighbour D–D distances play a role in the relative hole site occupations.

The structure of $Pr_6Fe_{13}AuD_{13}$ differs from the recently reported $Nd_6Fe_{13}GaD_{12.3}$ deuteride [12] with the same metal sublattice of the $Nd_6Fe_{13}Si$ type. Only the sites D1–D4 are occupied by D atoms while the D5 and D6 sites remain empty, resulting in a lower D content for $Nd_6Fe_{13}GaD_{12.3}$.

Acknowledgements

The possibility of collecting high quality diffraction data at the Swiss–Norwegian Beam Line, ESRF and the skillful assistance of Wouter van Beek is gratefully acknowledged.

References

[1] J. Allemand, A. Letand, J.M. Moreau, J.P. Nozières, R. Perrier de la Bâthie, J. Less-Common Met. 166 (1990) 73.
[2] F. Weitzer, A. Leithe-Jasper, P. Rogl, K. Hiebl, A. Rainbacher, G. Wiesinger, J. Friedl, F.E. Wagner, J. Appl. Phys. 75 (1995) 7745.
[3] O.M. Sichevich, R.V. Lapunova, A.N. Soboley, Yu.N. Grin, Ya.P. Yarmoluk, Sov. Phys. Crystallogr. 30 (1985) 627.
[4] C.H. de Groot, F.R. de Boer, K.H.J. Buschow, Phys. Rev. B 57 (1998) 11472.
[5] P. Schobinger-Papamantellos, K.H.J. Buschow, C.H. de Groot, F.R. de Boer, C. Ritter, F. Fauth, G. Boettger, J. Alloys Comp. 280 (1998) 44.
[6] C.H. de Groot, F.R. de Boer, K.H.J. Buschow, D. Hautot, G.J. Long, F. Grandjean, J. Alloys Comp. 233 (1996) 161.
[7] C.H. de Groot, F.R. de Boer, K.H.J. Buschow, D. Hautot, G.J. Long, F. Grandjean, J. Alloys Comp. 245 (1996) 188.

[8] D. Hautot, G.J. Long, F. Grandjean, C.H. de Groot, K.H.J. Buschow, Appl. Phys. 83 (1998) 1554.

[9] A. Leithe-Jasper, R. Skomski, Q. Qi, J.M.D. Coey, F. Weitzer, P. Rogl, J. Phys.: Condens. Matter 8 (1996) 3353.

[10] A.C. Larson, R.B. von Dreele, General Structure Analysis System (GSAS), LANSCE, MS-H 805 (1994).

[11] J. Rodríguez-Carvajal, Physica B 192 (1993) 55, The manual of FullProf can be obtained from a Web browser at ftp://bali.saclay.cea.fr/pub/divers/fullp/doc.

[12] V.A. Yartys, R.V. Denys, I.I. Bulyk, R.G. Delaplane, B.C. Hauback, J. Alloys Comp. 312 (1–2) (2000) 158.